Site-Specific Phosphorylation of ZYG-1 Regulates ZYG-1 Stability and Centrosome Number

Jeffrey C. Medley[1], Joseph DiPanni[1], Nahyun Yim[1], Brandon Sebou[1], Blake Shaffou[1], Evan Cramer[2], Colin Wu[2], Megan Kabara[1,3] and Mi Hye Song[1, 4]

[1]Department of Biological Sciences, and [2]Department of Chemistry, Oakland University, MI, USA.
[3]Connecticut Children's Medical Center in Hartford, CT, USA.
[4] Corresponding Author: Contact

Running title:
CK2-dependent Phosphorylation of ZYG-1 in Centrosome Assembly

Key words:
Casein Kinase II; CK2; *C. elegans*; Centrosome; Phosphorylation; ZYG-1

Corresponding author: Mi Hye Song

Biological Sciences, Oakland University, 344 Dodge Hall, 118 Library Drive, Rochester, MI

48309, USA.

Email: msong2@oakland.edu

Summary

Spindle bipolarity is critical for genomic integrity. Given that centrosome number often dictates mitotic bipolarity, tight control of centrosome assembly is vital for the fidelity of cell division. The kinase ZYG-1/Plk4 is a master centrosome factor that is integral for controlling centrosome number and is modulated by protein phosphorylation. While autophosphorylation of Plk4 has been extensively studied in other systems, the mechanism of ZYG-1 phosphorylation in *C. elegans* remains largely unknown. In *C. elegans*, Casein Kinase II (CK2) negatively regulates centrosome duplication through control of centrosome-associated ZYG-1 levels. In this study, we investigated ZYG-1 as a potential substrate of CK2 and the functional impact of ZYG-1 phosphorylation on centrosome assembly. First, we show that CK2 directly phosphorylates ZYG-1 *in vitro* and physically interacts with ZYG-1 *in vivo.* Intriguingly, depleting CK2 or blocking ZYG-1 phosphorylation at putative CK2 target sites leads to centrosome amplification. In the non-phosphorylatable (NP)-ZYG-1 mutant embryo, total ZYG-1 levels are increased, leading to elevated centrosomal ZYG-1 and downstream factors, providing a possible mechanism of the NP-ZYG-1 mutation to drive centrosome amplification. Moreover, inhibiting the 26S proteasome blocks degradation of the phospho-mimetic (PM)-ZYG-1, whereas the NP-ZYG-1 is partially resistant to proteasomal degradation. Our data suggest that site-specific phosphorylation of ZYG-1, in part by CK2, regulates ZYG-1 levels through proteasomal degradation to limit centrosome number. We provide a mechanism linking CK2 kinase activity to centrosome duplication through direct phosphorylation of ZYG-1, which is critical for the integrity of centrosome number.

Introduction

During cell division, equal distribution of chromosomes into each daughter cell is essential to maintain genomic integrity. As microtubule-organizing centers, centrosomes are critical for establishing mitotic bipolar spindles that ensure accurate transmission of genomic content[1]. Errors in centrosome number disrupt spindle bipolarity, leading to chromosome missegregation, and aberrant centrosomes are linked with human cancers and developmental defects[2,3]. To maintain proper centrosome numbers, centrosomes must duplicate only once per cell cycle through a process tightly regulated and coupled with the cell cycle[1,4].

Protein phosphorylation has emerged as a critical mechanism that controls the activity and abundance of key centrosome proteins[5]. In humans, the kinase Plk4 is a master regulator of centrosome biogenesis[6], and kinase activity of Plk4 is required for centrosome assembly via phosphorylation of other centrosome proteins. Plk4 phosphorylates the C-terminal STAN domain of STIL/Ana2/SAS-5, which promotes the direct binding of STIL/Ana2 to SAS-6 to initiate the procentriole formation[7–10]. In a subsequent step, Plk4 phosphorylates another site (S428) of STIL, promoting STIL binding to CPAP/SAS-4[11]. The *C. elegans* ZYG-1, the human Plk4-related kinase, is essential for centrosome duplication[12]. ZYG-1 localizes to the site of procentriole formation[13] and is required for centrosomal recruitment of SAS-5 and SAS-6[14–16]. ZYG-1, independently of its kinase activity, directly binds to SAS-6 to recruit SAS-6 and SAS-5 to nascent centrioles, whereas stable incorporation of SAS-6 into centrioles requires kinase activity of ZYG-1 via an unknown mechanism[17].

In centrosome assembly, the abundance of centrosome regulators is critical for centrosome number. It has been shown that levels of the human Plk4 are regulated by autophosphorylation and subsequent proteasomal degradation through SKP1-CUL1-F-box-protein (SCF)-TrCP/Slimb E3 ubiquitin ligase-dependent pathway[18,19]. The regulatory mechanism of Plk4/ZYG-1 abundance appears to be evolutionarily conserved. In *C. elegans, Drosophila,* and human cells, the $SCF^{Slimb/\beta TrCP}$ E3 ubiquitin ligase controls levels of Plk4/ZYG-1 through the conserved Slimb/βTrCP-binding motif (SBM)[19–22]. In *Drosophila* and human cells, autophosphorylation of the SBM triggers $SCF^{Slimb/\beta TrCP}$ binding to Plk4, promoting Plk4 degradation[18,23,24]. However, it remains elusive whether autophosphorylation of ZYG-1 *in C. elegans* has a similar role in $SCF^{Slimb/\beta TrCP}$-mediated degradation of ZYG-1. Several *C. elegans* genes have been identified that regulate ZYG-1 activity. Genetic screens for suppressors of *zyg-1* revealed that ZYG-1 activity in centrosome assembly is modulated through several mechanisms, including transcription, RNA

binding, proteolysis, and protein phosphorylation[25–29]. Studies in *C. elegans* have shown that protein phosphorylation influences cellular and centrosomal levels of ZYG-1, which is critical for normal centrosome number and microtubule-nucleating activity[25,29–31]. PP2A$^{SUR-6/B55}$ exhibits a strong genetic interaction with ZYG-1 and SAS-5, and PP2A$^{SUR-6/B55}$-dependent dephosphorylation positively affects abundance of ZYG-1 and SAS-5, suggesting that PP2A$^{SUR-6/B55}$-dependent dephosphorylation stabilizes ZYG-1 and SAS-5 by protecting these proteins from proteasomal destruction[31]. It remains unknown what kinase counteracts PP2A$^{SUR-6/B55}$-mediated dephosphorylation of these centrosome proteins in *C. elegans,* whereas PP2A-dependent dephosphorylation has been proposed to counteract autophosphorylation of Plk4 and stabilizes Plk4 in humans and flies[32].

In *C. elegans,* Casein Kinase II (CK2) has been shown to negatively regulate centrosome duplication[25]. CK2 typically functions as a tetrameric holoenzyme comprising two catalytic (CK2α) and two regulatory (CK2β) subunits. The *C. elegans* genome contains the *kin-3* and *kin-10* genes that encode for the CK2α and CK2β subunits, respectively[33,34], and CK2 functions in various cellular processes[35–43] including microRNA targeting[42] and cell division[25]. CK2 is an evolutionarily conserved serine/threonine protein kinase and targets numerous substrates (>500) in diverse cellular processes[44,45]. In human cells, it has been shown that CK2 activity is elevated in both tumor cells and normal proliferating cells[46,47], and deregulated CK2α activity results in centrosome amplification by an unknown mechanism[48].

In *C. elegans*, CK2 negatively regulates centrosome duplication through control of centrosome-associated ZYG-1 levels[25]. However, specific substrate(s) of CK2 and the sites of phosphorylation in centrosome assembly have not been identified yet. In this study, we investigated ZYG-1 as a potential substrate of CK2 and examined the functional impact of site-specific phosphorylation of ZYG-1 on centrosome assembly *in vivo*. Blocking phosphorylation of ZYG-1 at potential CK2 target sites phenocopies loss of CK2 in centrosome assembly. Non-phosphorylatable ZYG-1 stabilizes ZYG-1, promoting centrosome amplification. Our findings suggest that multi-site phosphorylation of ZYG-1, likely by CK2, regulates ZYG-1 stability and is critical for the integrity of centrosome number in *C. elegans* embryos.

Results

Loss of CK2 Results in Extra Centrosomes

It has been shown that *kin-3(RNAi)*-mediated partial knockdown of CK2 does not significantly impact embryonic development[25,42]. By contrast, embryos further depleted of KIN-3, when animals were treated with *kin-3(RNAi)* for extended hours (40-48 hours), were partially inviable with various cell division phenotypes[25]. Remarkably with further knockdown of KIN-3/CK2, these embryos produced tripolar spindles (**Fig 1A, S1A**). In *C. elegans*, sperm provides a pair of centrioles to the embryo during fertilization. During the first mitosis, the paternal centriole pair segregates and duplicates, then two centrosomes establish bipolar spindles. Live imaging shows that *kin-3(RNAi)*-treated embryos undergo normal cytokinesis at the first mitosis and form tripolar spindles at the second mitosis (**Fig S1A**), suggesting that extra centrosomes likely arise from centrosome overduplication. These observations illustrate that inhibiting CK2 kinase activity results in centrosome amplification in *C. elegans* embryos, indicating that CK2 kinase activity is critical for the integrity of centrosome number, possibly through phosphorylation of one or more centrosome proteins.

CK2 directly phosphorylates ZYG-1 *in vitro*

While CK2 kinase activity influences centrosome assembly in *C. elegans* embryos[25], we do not know the specific substrate(s) and sites phosphorylated by CK2 that are critical for centrosome assembly. A compelling candidate is the kinase ZYG-1, a master regulator of centrosome duplication[12]. In *C. elegans*, it has been shown that increased centrosomal ZYG-1 or hyperactive ZYG-1 leads to extra centrosomes in early embryos[20,29] and seam cells[49]. Because CK2 kinase activity negatively regulates centrosome duplication by controlling ZYG-1 levels at centrosomes[25], we hypothesized CK2 directly phosphorylates ZYG-1, and that the phosphorylation state of ZYG-1 influences ZYG-1 activity in regulating centrosome assembly. We first tested whether the kinase CK2 can phosphorylate ZYG-1 *in vitro* (**Fig 1B)**. Since the *C. elegans* kinase ZYG-1 is shown to be autophosphorylated *in vitro*[12], we used the kinase-dead ZYG-1 (KD-ZYG-1^{K41M}; [12]) as a substrate to eliminate auto-phosphorylated ZYG-1 for *in vitro* kinase assay. Autoradiograph illustrates that CK2 phosphorylates KD-ZYG-1^{K41M,} but the CK2 kinase inhibitor (TBB) blocks phosphorylation of KD-ZYG-1^{K41M} by CK2. Furthermore, our immunoprecipitation (IP) assays using embryonic lysates suggests a physical interaction between 2xMyc::ZYG-1 and KIN-3::V5 *in vivo*[20,50] (**Fig 1C**). Collectively, our data support a hypothesis that CK2 directly phosphorylates ZYG-1.

CK2 Consensus Sites in the L1 Domain of ZYG-1

CK2 is a serine/threonine protein kinase that favors substrates containing acidic residues downstream of the phosphorylation site[51,52]. For prediction of potential phosphorylation residues,

we used *in silico* approaches (KinasePhos3.0[53]; and GPS 5.0[54]) and identified several ZYG-1 residues at S279, S280, S620 and T621 showing the highest likelihood of CK2 consensus motifs (**Table S1**). These potential CK2 target sites are located in two distinct regions: S279/S280 in the Linker 1 (L1) domain and S620/T621 in the Linker 2 (L2) domain (**Fig 2A**). The sequence alignments illustrate that S279 and S280 exhibit a strong evolutionary conservation (**Fig S2A**), but S620 and T621 have a weaker conservation (**Fig S2B**) within the *Caenorhabditis* genus. Based on the sequence conservation, we focused on S279 and neighboring serine residues within the L1 domain critical for ZYG-1 function in centrosome assembly[17,20]. S279 is located within a cluster of serine residues (aa260-285: **Fig 2A**). Each serine residue in this cluster conforms to the minimal CK2 consensus motif and is highly conserved throughout the *Caenorhabditis* genus (**Fig S2A)**. Given that the *C. elegans* ZYG-1 is evolutionarily divergent from Plk4 orthologs, S279 and adjacent serine sites are not conserved in the human Plk4 although Plk4 contains several serine/threonine residues that conform to the CK2 consensus motif (**Table S2**). Intriguingly, this ZYG-1 region (aa260-280) coincides with the direct binding domain of ZYG-1 to SAS-6[17] highlighting the functional significance of this ZYG-1 region critical for centrosome duplication. Herein, we will refer to this region as the ZYG-1:4S.

To test whether CK2 phosphorylates ZYG-1 at these sites, we performed *in vitro* kinase assay using the ZYG-1 peptides (aa260-285) containing four serine residues as a substrate (**Fig S2C**). Autoradiogram of thin layer chromatography (TLC) displays that CK2 phosphorylates the wild-type ZYG-1 peptide, but not the ZYG-1:4A peptide where four sites (S273, S279, S280, and S285) were replaced to alanine. By contrast, the CK2 inhibitor TBB decreased CK2-dependent phosphorylation of the ZYG-1 peptide.

Furthermore, we performed mass spectrometry analysis following *in vitro* kinase reactions using the ZYG-1 peptide substrate and CK2, confirming that at least one of two serine residues (S279 and S280) in this ZYG-1 peptide can be phosphorylated by CK2 reproducibly (**Fig S2D**[55]). Our data suggest CK2 directly phosphorylates at least one serine residue within the ZYG-1 L1 domain.

Non-phosphorylatable ZYG-1 Mutation Leads to Centrosome Amplification

To address the functional impacts of site-specific phosphorylation of ZYG-1 *in vivo*, we used CRISPR/Cas9 editing to mutate S279 to a non-phosphorylatable (NP) alanine, termed ZYG-1^{S279A} and a phospho-mimetic (PM) aspartate, termed ZYG-1^{S279D} at the endogenous locus (**Fig 2A**). In parallel, we simultaneously mutated all four serine residues (S273, S279, S280 and S285) to alanine, termed ZYG-1^{4A}, or aspartate, termed ZYG-1^{4D}. The homozygous ZYG-1 phospho-

mutants we generated were mostly viable, with ZYG-1^{4A} and ZYG-1^{4D} mutants producing a low rate of embryonic lethality (**Table 1**). Since *kin-3(RNAi)*-mediated inhibition of CK2 leads to tripolar spindle formation (**Fig 1A**), we speculated that mutating a subset of CK2 target sites to non-phosphorylatable alanine (NP-ZYG-1 mutations) should at least partially phenocopy loss of CK2, including extra centrosomes. We first observed centrosome behavior to determine how the phosphorylation state of ZYG-1 affected centrosome duplication (**Fig 2B,S3**). Intriguingly, we observed extra centrosomes in ZYG-1^{4A} mutant embryos, starting at the first mitosis and later cell divisions (~30%, n>100 embryos). Extra centrosomes are reminiscent phenotypes arising from Plk4 overexpression[6], suggesting the ZYG-1^{4A} mutation upregulates ZYG-1 activity and that hyperactive ZYG-1 results in centrosome amplification. Furthermore, we observed various cell division phenotypes in the ZYG-1^{4A} mutant embryos (**Fig S3A**), including DNA missegregation, cytokinesis failure, detached centrosomes and expanded PCM morphology, similar to phenotypes observed in embryos depleted of CK2[25]. These observations together show that the NP-ZYG-1^{4A} mutation phenocopies loss of CK2 during *C. elegans* embryogenesis. On the contrary, the ZYG-1^{4D} mutation led to monopolar spindle formation in one-cell and later-stage embryos (~30%, n>100) (**Fig 2B,S3C**), indicating that the PM-ZYG-1^{4D} mutation downregulates ZYG-1 activity and impair centrosome duplication during spermatogenesis and mitotic divisions.

Non-phosphorylatable ZYG-1 Leads to Elevated ZYG-1 Levels

Given that inhibiting CK2 kinase activity leads to elevated centrosomal ZYG-1[25], we examined how the NP-and PM-ZYG-1 mutations affected ZYG-1 levels at centrosomes. To facilitate this assay, we introduced a 2xMyc tag at the endogenous N-terminal *zyg-1* locus by CRISPR/Cas9 editing[20]. By immunostaining embryos with anti-Myc, we quantified centrosome-associated 2xMyc::ZYG-1 fluorescence intensity during the first mitosis (**Fig 2C**). The NP-ZYG-1^{4A} still localizes to centrosomes, suggesting alanine replacements at these serine sites did not impair ZYG-1 loading to centrosomes. Quantitative immunofluorescence (IF) revealed that ZYG-1^{4A} mutant embryos exhibit significantly increased 2xMyc::ZYG-1 signals at centrosomes (1.47±0.45 fold, $p<0.001$), but ZYG-1^{4D} mutants had decreased levels (0.81±0.28 fold, $p<0.01$), compared to wild-type controls (1.00 ± 0.20 fold). At the first metaphase, similar trends were observed (**Fig S4A**). Our data illustrate that the phosphorylation state of ZYG-1 affects its protein levels at centrosomes.

Increased levels of cellular ZYG-1 might account for elevated centrosomal ZYG-1 in the NP-ZYG-1 mutants. Following Myc-pulldown using embryonic lysates expressing 2xMyc::ZYG-1, we could

detect Myc-tagged ZYG-1, with significantly increased levels (1.98±0.51-fold, $p<0.0001$, n=6) of 2xMyc::ZYG-1 in ZYG-1^{4A} embryos, and reduced levels (0.51±0.19-fold, $p<0.0001$, n=6) in ZYG-1^{4D} mutants (**Fig 2D**). Our quantitative immunoblot supports a model where the NP-ZYG-1 is hyperstabilized, leading to increased levels of cellular ZYG-1 and, thereby more ZYG-1 loaded to centrosomes.

Non-phosphorylatable ZYG-1 Restores Centrosome Duplication in *zyg-1(it25)*

Depletion of CK2 restores centrosome duplication and embryonic viability to *zyg-1(it25)* mutants[25]. We thus asked if the NP-ZYG-1 mutation, mimicking loss of CK2, could produce similar effects on *zyg-1(it25)* mutants. In this scenario, the NP-ZYG-1 mutation should restore embryonic viability and centrosome duplication to *zyg-1(it25)* mutants. To test this, we used CRISPR/Cas9 editing and introduced equivalent phospho-mutations to *zyg-1(it25)* mutants at the endogenous locus. In the temperature-sensitive *zyg-1(it25)* mutant embryos grown at the restrictive temperature 24°C, centrosome duplication fails during the first cell cycle, resulting in monopolar spindles at the second mitosis and 100% embryonic lethality[12]. Remarkably, the ZYG-1^{4A} mutation led to a significant restoration (>10-fold) of embryonic viability, and the ZYG-1^{S279A} mutation produced a relatively moderate but significant restoration (3.5-fold) to *zyg-1(it25)* mutants at the semi-restrictive temperature conditions (**Table 1, Fig 3A**). By contrast, the ZYG-1^{4D} and ZYG-1^{S279D} mutations produced opposite effects on *zyg-1(it25)* mutants (**Table 1, Fig 3A**). These results suggest that the NP-ZYG-1 mutation upregulates ZYG-1 activity, compensating for the hypomorphic ZYG-1 function in *zyg-1(it25)* mutants while the PM-ZYG-1 mutations have the opposite effect.

Given that ZYG-1 is essential for centrosome duplication, restoring embryonic viability to *zyg-1(it25)* mutants likely results from successful centrosome duplication. To examine how ZYG-1 phospho-mutations affected centrosome duplication in the *zyg-1(it25)* mutant, we scored for bipolar spindle formation during the second mitosis (**Fig 3B**). Consistent with the genetic suppression, both NP-ZYG-1^{S279A} and ZYG-1^{4A} mutations restored bipolar spindles to *zyg-1(it25)* mutants (13.8±6.2%), with the ZYG-1^{4A} mutation (77.7±10%) exhibiting a higher rate of bipolar spindles than the ZYG-1^{S279A} mutation (38.1±12%). Conversely, both PM-ZYG-1 mutations (ZYG-1^{S279D} and ZYG-1^{4D}) decreased bipolar spindle formation (6±3.6% and 0%, respectively). Similar to loss of CK2, it appears the NP-ZYG-1 mutations enhance ZYG-1 activity, thereby restoring centrosome duplication and embryonic viability to *zyg-1(it25)* mutants, whereas the PM-ZYG-1 diminishes ZYG-1 activity and aggravate *zyg-1(it25)* phenotypes.

Increased levels of centrosomal ZYG-1 in ZYG-1^{4A} mutants may explain suppression of *zyg-1(it25)* phenotypes by the NP-ZYG-1 mutation. To directly test this, we compared centrosomal ZYG-1 levels in *zyg-1(it25)* mutant backgrounds (**Fig 3C**). Quantitative IF using anti-ZYG-1[56] illustrate significantly increased levels of centrosomal ZYG-1 in ZYG-1^{4A}: *zyg-1(it25)* (1.45±0.33-fold, p<0.001) and ZYG-1^{S279A}: *zyg-1(it25)* (1.26±0.43-fold, p<0.001) embryos, compared to *zyg-1(it25)* controls (1.00±0.26-fold) at the first anaphase. Notably, the ZYG-1^{4A} mutation produced a stronger impact on centrosomal ZYG-1 levels than the ZYG-1^{S279A} mutation, consistent with more robust *zyg-1* suppression by ZYG-1^{4A} than the ZYG-1^{S279A} mutation (**Fig 3A,B and Table1**). Conversely, reduced centrosomal ZYG-1 levels were observed in the ZYG-1^{4D}: *zyg-1(it25)* (0.75±0.42-fold, p<0.001) and ZYG-1^{S279D}: *zyg-1(it25)* (0.67±0.33-fold, p<0.001) mutants at the first anaphase. Together, our results suggest that phosphorylation of ZYG-1 at multiple sites regulates centrosomal ZYG-1 levels, thereby influencing ZYG-1 activity in centrosome assembly.

ZYG-1 Phosphorylation Affects Centrosomal Loading of Downstream Centrosome Factors

In the molecular hierarchy of centrosome assembly, SPD-2 acts upstream and promotes centrosomal targeting of ZYG-1 via direct electrostatic interaction[57], and ZYG-1 is required for centrosomal recruitment of downstream centrosome factors, SAS-5, SAS-6 and SAS-4[14,17]. Then, elevated centrosomal ZYG-1 in ZYG-1^{4A} mutants might further enhance centrosomal recruitment of downstream factors, leading to centrosome amplification. Alternatively, the phosphorylation state of ZYG-1 could affect interaction with other centrosome factors, positively or negatively.

Quantitative IF at the first anaphase illustrates that NP-ZYG-1^{4A} mutant embryos exhibit increased levels of centrosomal SAS-6 (1.26±0.31 fold, p<0.001), while ZYG-1^{4D} mutant embryos show reduced SAS-6 levels (0.73±0.17 fold, p<0.01), compared to wild-type controls (1.00±0.28 fold) (**Fig 4A**). An increase of SAS-6 in NP-ZYG-1^{4A} mutant centrosomes might result from elevated centrosomal ZYG-1. Alternatively, the phosphorylation state of ZYG-1 could affect the ZYG-1-SAS-6 binding affinity through charge changes, given that the phosphorylation cluster (ZYG-1:4S) coincides with the ZYG-1 domain that directly binds to SAS-6 through electrostatic attraction[17]. By quantitative immunoblot following Myc-IP (**Fig S2E**), we compared relative levels of SAS-6 associated with 2xMyc::ZYG-1 in Myc-IP. Both Myc-pulldowns of ZYG-1^{4A} and ZYG-1^{4D} show the ratio of SAS-6/2xMyc::ZYG-1 higher than controls, implying that the phosphorylation states of ZYG-1 do not adversely affect the ZYG-1-SAS-6 binding affinity. Thus, it seems more likely that elevated centrosomal ZYG-1 in ZYG-1^{4A} mutants further enhances SAS-6 recruitment to centrosomes.

ZYG-1 is also required for centrosomal SAS-5 loading, and SAS-5 and SAS-6 are co-dependent for centrosomal localization[15]. Consistent with SAS-6, we observed significantly increased SAS-5 in ZYG-1^{4A} mutant centrosomes (1.20±0.43 fold, p<0.001), but decreased levels in ZYG-1^{4D} centrosomes (0.73±0.29 fold, p<0.001), compared to controls (1.00 ± 0.40 fold) (**Fig 4B,C**). For centrosomal SAS-4, we observed similar trends, with a significant increase in ZYG-1^{4A} mutants (1.20±0.43 fold, p<0.001) but a decrease in ZYG-1^{4D} mutants (0.73±0.29 fold, p<0.001) (**Fig 4B,D**). We also quantified centrosomal levels of SAS-4, 5, and 6 at the first metaphase, showing similar trends in ZYG-1 phospho-mutants (**Fig S4B-D**).

Finally, we asked how ZYG-1 phosphorylation influences centrosomal levels of SPD-2 that functions upstream of ZYG-1 and is required for centrosomal recruitment of ZYG-1[14,58]. The interaction between SPD-2 and ZYG-1 also relies on electrostatic interactions between the N-terminal SPD-2 acidic region and the ZYG-1 cryptic polo box (CPB) basic patch (aa350-560[57]). As the ZYG-1 L1 domain bridges the kinase and CPB domains, phosphorylation of the ZYG-1:4S may affect the interaction between ZYG-1 and SPD-2, influencing centrosomal recruitment of ZYG-1. Using strains expressing SPD-2::2xHA at the endogenous locus, we quantified total centrosomal SPD-2::2xHA signals in ZYG-1 phospho-mutants. In contrast to ZYG-1 downstream factors, we found no significant changes in centrosomal SPD-2 levels in ZYG-1^{4A} (1.11±0.58 fold, p=0.49) and ZYG-1^{4D} mutants (1.08±0.56 fold, p=0.26) compared to controls (1.00 ± 0.19 fold) at the first anaphase (**Fig 4E**), and similar trends at the metaphase (**Fig S4E,F**). Furthermore, the phosphorylation state of ZYG-1 did not significantly affect centrosomal levels of the PCM component TBG-1/γ-tubulin during the first mitosis (**Fig S4G**). Given ZYG-1 acting downstream of SPD-2 in centrosome assembly, our results are consistent with a genetic hierarchy where ZYG-1 phospho-mutations had no significant effect on centrosomal SPD-2.

Collectively, our data illustrate that the phosphorylation state of ZYG-1 affects centrosomal recruitment of downstream centrosome proteins, partially explaining how phosphorylation of ZYG-1 influences centrosome number in the *C. elegans* embryo.

CK2-dependent Phosphorylation of ZYG-1

If CK2 targets one or more serine residues in the ZYG-1:4S region (**Fig 2A**), ZYG-1 phospho-mutants should be less responsive to CK2 depletion compared to controls. However, if CK2 targets none of the serine residues in this region, ZYG-1 phospho-mutants should be as responsive to CK2 depletion as controls. For the latter, combining CK2 depletion with the ZYG-

1^{4A} mutation should show an additive effect. To test this, we used *kin-3(RNAi)* to knockdown KIN-3, the catalytic subunit of CK2, and assayed for bipolar spindle formation in *zyg-1(it25)* genetic backgrounds at the second mitosis (**Fig 5A,B**). As shown in *zyg-1(it25)* controls[25], *kin-3(RNAi)* significantly increased bipolar spindle formation by 6.7-fold, compared to control RNAi. For ZYG-1^{4A}: *zyg-1(it25)* mutants, control RNAi and *kin-3(RNAi)*-treated embryos produced 75±7.8% and 98±2.4% of bipolarity, respectively, showing that *kin-3(RNAi)* led to only a small (1.3-fold) increase in bipolarity compared to control RNAi. In ZYG-1^{4D}: *zyg-1(it25)* mutants, control RNAi produced nearly zero bipolarity (0.4±1.1%), and *kin-3(RNAi)* led to 16.1±3.3% of bipolarity, much lower than expected to be additive (~44%). These results indicate that the PM-ZYG-1^{4D} mutant is partially resistant to CK2 knockdown, further supporting that CK2 phosphorylates one or more serine residues in the ZYG-1:4S.

Additionally, if the ZYG-1:4S region contains the only target sites phosphorylated by CK2, *kin-3(RNAi)* should not affect % bipolarity in ZYG-1^{4A}: *zyg-1(it25)* mutants. On the contrary, *kin-3(RNAi)* led to a moderate but noticeable increase of bipolarity in both *zyg-1(it25)* phospho-mutants (**Fig 5B**), implying that CK2 likely targets additional ZYG-1 residues or other substrates that influence centrosome assembly directly or indirectly.

PP2A$^{SUR-6/B55}$ May Counteract CK2 to Balance the Phosphorylation State of ZYG-1

In *C. elegans*, the kinase CK2 and the phosphatase PP2A$^{SUR-6/B55}$ play opposing roles in centrosome duplication; CK2 as a negative regulator[25] and PP2A$^{SUR-6/B55}$ as a positive regulator[30,31]. Inhibiting CK2 increases centrosomal ZYG-1 levels[25], whereas loss of PP2A$^{SUR-6/B55}$ decreases cellular ZYG-1 levels[31], suggesting that CK2 and PP2A$^{SUR-6/B55}$ counteract to regulate centrosome assembly via controlling ZYG-1 levels. Intriguingly, serine residues in the ZYG-1:4S conform to not only CK2 phosphorylation sites[52] but also minimal PP2A$^{SUR-6/B55}$ consensus motifs[59,60].

Loss of PP2A$^{SUR-6/B55}$ has been shown to enhance monopolar spindles in *zyg-1(it25)* mutants, in contrast to the impact of CK2 depletion[25,31]. A recent study in *C. elegans* also showed that *kin-3* suppresses *sur-6,* encoding the SUR-6/B55 regulatory subunit of PP2A, in centrosome duplication[61]. Our results indicate that the PM-ZYG-1^{4D} mutation enhances monopolar spindles in *zyg-1(it25)* mutants, whereas the NP-ZYG-1^{4A} mutation had an opposite effect (**Fig 3B**), which led us to speculate that PP2A$^{SUR-6/B55}$ might dephosphorylate the ZYG-1:4S and counteract CK2 to balance the phosphorylation state of ZYG-1. If PP2A$^{SUR-6/B55}$ dephosphorylates one or more serine residues in the ZYG-1:4S, our phospho-mutants should be at least partially resistant to

SUR-6 inhibition. We treated animals with *sur-6(RNAi)* to partially deplete PP2A$^{SUR-6/B55}$ and observed centrosome duplication (**Fig 5D**). Consistent with the previous work[31], *sur-6(RNAi)* decreased bipolarity by 9-fold in the *zyg-1(it25)* control, compared to control RNAi. In the ZYG-1^{4A}: *zyg-1(it25)* mutants, *sur-6(RNAi)* produced only a minor decrease in bipolarity (34±7.2%, 2-fold) relative to control RNAi (75±7.8%), indicating a partial resistance of the ZYG-1^{4A} to PP2A$^{SUR-6/B55}$ knockdown. Thus, PP2A$^{SUR-6/B55}$ likely targets the ZYG-1:4S. Our collective data suggest that CK2 and PP2A$^{SUR-6/B55}$ target one or more shared serine residues in the ZYG-1:4S, and they counteract to balance the phosphorylation state of ZYG-1, providing a regulatory mechanism to keep ZYG-1 levels at the above threshold level to support centrosome duplication.

Phosphorylation of ZYG-1 Promotes Proteasomal Degradation

Collectively, our data support a model where the phosphorylation state of ZYG-1 regulates overall ZYG-1 levels, likely through the control of protein stability. One possible mechanism is that phosphorylated ZYG-1 in the ZYG-1:4S is subject to proteasomal degradation, and when dephosphorylated, ZYG-1 is protected from degradation and stabilized. To test if ZYG-1 phosphorylation in the ZYG-1:4S promotes proteasomal degradation, we treated ZYG-1 phospho-mutant *zyg-1(it25)* animals with *rpt-4(RNAi)* to deplete the proteasome activity partially, at a condition that allows completion of meiotic and early mitotic cycles[31]. We then asked how inhibiting the 26S proteasome affected the activity of ZYG-1^{4A} and ZYG-1^{4D} in centrosome duplication (**Fig 5A,D**). If *rpt-4(RNAi)* partially blocked degradation of the phospho-mimetic ZYG-1 (ZYG-1^{4D}), *rpt-4(RNAi)* should protect the unstable ZYG-1^{4D} at least partially from degradation, and then stabilized ZYG-1^{4D} should restore bipolarity in ZYG-1^{4D}: *zyg-1(it25)* embryos.

First, we confirmed that in *zyg-1(it25)* controls, *rpt-4(RNAi)* significantly increased bipolar spindle formation by 3.4-fold, compared to control RNAi, consistent with previous work[20]. As expected, in ZYG-1^{4D}: *zyg-1(it25)* mutants, compared to control RNAi, *rpt-4(RNAi)* produced a stark increase in bipolar spindles (49±14%, 33.5-fold), close to the % bipolarity observed in the ZYG-1^{4A}: *zyg-1(it25)* mutants (59±10%). By contrast, in ZYG-1^{4A}: *zyg-1(it25)* mutants, *rpt-4(RNAi)* produced only a small increase (1.4-fold) compared to control RNAi. Together, *rpt-4(RNAi)* leads to a remarkable stabilization of the ZYG-1^{4D} but only a minor effect on the ZYG-1^{4A}, suggesting that inhibiting the 26S proteasome blocks proteasomal degradation of ZYG-1^{4D}, whereas ZYG-1^{4A} is partially resistant to proteasomal degradation. It seems plausible that phosphorylated ZYG-1 is subject to proteasomal destruction, triggered by CK2-dependent phosphorylation at the ZYG-1:4S. These results support a model where site-specific phosphorylation of ZYG-1 by CK2

regulates ZYG-1 stability through the 26S proteasome, providing a critical mechanism for the integrity of centrosome number in *C. elegans* embryos.

Discussion

CK2 kinase activity is critical for the integrity of centrosome number

In this study, we report that inhibiting CK2 leads to centrosome amplification (**Fig 1A**), indicating CK2 kinase activity is critical for the integrity of centrosome number. Given that CK2 negatively regulates centrosome duplication by controlling ZYG-1 levels at centrosomes[25], we hypothesized that CK2 directly phosphorylates ZYG-1 and phosphorylation of ZYG-1 by CK2 influences ZYG-1 activity in centrosome assembly. First, we show that CK2 directly phosphorylates kinase-dead ZYG-1 *in vitro,* and ZYG-1 physically interacts with CK2 *in vivo* (**Fig 1B,C**). Given the supporting evidence of ZYG-1 as a potential substrate of CK2, we examined the functional impact of phosphorylation of ZYG-1 at the putative CK2 target sites. Our *in silico* analysis identified several serine residues in ZYG-1 that conform to the CK2 consensus motif (**Table S1**). Here, we focused on four serine sites, including S279 and adjacent serine residues (ZYG-1:4S) in the ZYG-1 L1 domain (**Fig 2A**), which is critical for centrosomal ZYG-1 loading and the direct binding to SAS-6[17,57], and well conserved in closely related nematodes (**Fig S2A**). By generating the phospho-mutant *zyg-1* strains edited at the putative CK2 target sites (ZYG-1:4S), we examined the functional impact of ZYG-1 phosphorylation in centrosome assembly *in vivo*. Our functional analyses reveal that mutating four serine residues simultaneously produces much more potent effects on ZYG-1 activity than the S279 single mutation, indicating that S279 and at least one additional serine in the ZYG-1:4S are phosphorylated *in vivo*. Furthermore, genetic and mass spectrometry analysis suggest that CK2 has at least one target site in the ZYG-1:4S *in vivo* (**Fig 5B**) and CK2 phosphorylates at least one serine between S279 and S280 *in vitro* (**Fig S2D**). Together, our results are consistent with the idea that CK2 directly phosphorylates the ZYG-1:4S, and phosphorylation of ZYG-1 at multiple sites, including CK2 target site(s), regulates ZYG-1 activity.

The phosphorylation state of ZYG-1 regulates ZYG-1 stability

Our collective data strongly support the NP-ZYG-1 mutations phenocopy loss of CK2. The NP-ZYG-1 mutations restore centrosome duplication and embryonic viability to the hypomorphic *zyg-1(it25)* mutants, indicating hyperactive ZYG-1. Remarkably, the NP-ZYG-1 mutations lead to centrosome amplification, reminiscent of the phenotype from overexpression of Plk4/ZYG-1. Consistently, total ZYG-1 levels are significantly increased in the NP-ZYG-1 embryos, leading to

elevated levels of ZYG-1 and downstream factors at centrosomes, providing a possible mechanism of the NP-ZYG-1 mutation to drive centrosome amplification.

Moreover, our data imply that the PM-ZYG-1 is stabilized by inhibition of the 26S proteasome, and the NP-ZYG-1 is partially resistant to the 26S proteasome, supporting our model where site-specific phosphorylation of ZYG-1 regulates ZYG-1 stability through proteasomal degradation. Thus, counteraction between CK2 and a phosphatase, possibly $PP2A^{B55}$ based on our analysis discussed below, appears to balance the phosphorylation state of ZYG-1, regulating ZYG-1 levels through proteolysis to limit the centrosome number.

Regulation of CK2-dependent phosphorylation of ZYG-1

Since the kinase CK2 is constitutively active[62], a refractory mechanism to counteract CK2 should be available for balancing the phosphorylation state of ZYG-1. One mechanism could be through dephosphorylation of ZYG-1 by protein phosphatase. In *C. elegans*, $PP2A^{SUR\text{-}6/B55}$ positively regulates ZYG-1 levels[31], which appears to be conserved in *Drosophila* where $PP2A^{Twins/B55}$ has been proposed to stabilize Plk4 by counteracting autophosphorylation[32]. Serine residues in the ZYG-1:4S conform to the $PP2A^{B55}$ consensus motif surrounded by polybasic residues[59,60] (**Fig 2A,S2A**). Thus, it seems plausible that $PP2A^{SUR\text{-}6/B55}$ may counteract CK2-dependent phosphorylation at the ZYG-1:4S to stabilize ZYG-1. Another possibility is through the substrate availability that restricts phosphorylation of ZYG-1. ZYG-1 undergoes stepwise interactions with centrosome proteins in the process of centrosome biogenesis[17,57]. CK2 target sites in ZYG-1 could be masked or competed by another protein, which blocks CK2 targeting. Such a mechanism has been described in human cells where Plk4 and CDK-1 compete for the binding to STIL/Ana2/SAS-5, providing the temporal regulation of STIL phosphorylation[63]. Alternatively, efficient CK2 targeting may require conformational changes of ZYG-1. In human cells, Plk4 binding to STIL/Ana2/SAS-5 triggers Plk4 kinase activity[10]. Likewise, ZYG-1 binding to the other centrosome factor could induce ZYG-1 conformation optimal for CK2 targeting. Since the ZYG-1:4S resides within the ZYG-1 binding domain to SAS-6[17], the ZYG-1 binding to SAS-6 or another centrosome factor could induce conformational changes of ZYG-1, promoting or blocking CK2 targeting.

Mechanism of ZYG-1 Phosphorylation

In *C. elegans*, the mechanism of ZYG-1 phosphorylation remains largely unknown, while autophosphorylation of Plk4 has been extensively studied in humans and flies. Plk4 autophosphorylates a cluster of residues in the L1 domain, and autophosphorylation of Plk4 is pivotal for both its kinase activation and stability[18,19,23,24,64,65], providing a mechanism for proper

centrosome number. In this study, we describe a cluster of serine residues in the ZYG-1 L1 domain (ZYG-1:4S) that regulates ZYG-1 stability, analogous to the mechanism of Plk4 autophosphorylation. Both Plk4 and ZYG-1 have a conserved SBM responsible for $SCF^{Slimb/\beta TrCP}$-mediated proteolysis[18–20,23,24]. For Plk4, activation of the SBM phosphodegron is achieved by autophosphorylation[19,23,24]. While the ZYG-1 SBM plays a conserved role in regulating its stability[20], it remains unclear if ZYG-1 autophosphorylation provides a similar mechanism. The ZYG-1 SBM (aa334-339), located outside the ZYG-1:4S (aa273-280), does not conform to the CK2 consensus motif, implicating that the ZYG-1 SBM is unlikely phosphorylated by CK2. Given that ZYG-1 is autophosphorylated *in vitro*[12], it is tempting to speculate that autophosphorylation of the ZYG-1 SBM promotes SCF-mediated destruction via a conserved mechanism. Thus, it seems likely that phosphorylation of ZYG-1 at the ZYG-1:4S regulates ZYG-1 stability independently of $SCF^{Slimb/\beta TrCP}$-mediated pathway. In *C. elegans*, centrosomal ZYG-1 levels are regulated by the anaphase promoting complex/cyclosome $(APC/C)^{FZR-1}$ E3 ubiquitin ligase in parallel with $SCF^{Slimb/\beta TrCP}$ [20]. In humans, Plk4 levels are also regulated by another E3 ubiquitin ligase, Mib1[66], and by TEC tyrosine kinase-dependent phosphorylation[67], illustrating that Plk4/ZYG-1 stability is regulated through multiple pathways. Thus, CK2-dependent phosphorylation of ZYG-1 likely provides an additional layer of regulatory mechanism to fine-tune ZYG-1 activity in centrosome assembly.

In summary, our study provides important insights into the mechanism of ZYG-1 phosphorylation and CK2 kinase activity that ensure proper centrosome assembly in proliferating cells. This study is the first to report that CK2 directly phosphorylates ZYG-1/Plk4 in any organism. As the *C. elegans* ZYG-1 is highly divergent from Plk4 orthologs in other organisms[68,69], it will be interesting to test whether CK2 directly phosphorylates Plk4 orthologs in other organisms. In human cells, it has been shown that CK2 activity is elevated in both cancer cells and normal proliferating cells[46,47], and dysregulation of CK2α activity is shown to cause centrosome amplification. However, specific targets in this process remain unknown[48]. In the context of our findings, it is intriguing to speculate that CK2 may influence centrosome assembly through direct phosphorylation of Plk4, perhaps by a similar regulatory mechanism described in *C. elegans*. Whether CK2 directly phosphorylates Plk4 and how aberrant CK2 activity is linked to abnormal centrosome number in human cells remain important questions for future studies.

Table 1. Genetic Analysis

Strain	°C	% Embryonic Viability (ave ± s.d.)	n (progeny)
wild-type (N2)		100 ± 0	1803
ZYG-1^{S279A}		98.7 ± 2.5	1542
ZYG-1^{4A}		90.4 ± 5.0	2052
ZYG-1^{S279D}		99.0 ± 3.3	1669
ZYG-1^{4D}		98.6 ± 1.7	1718
zyg-1(it25)	22.5	8.8 ± 8.2	1275
ZYG-1^{S279A}*: zyg-1(it25)*		31.1 ± 19.9	1301
ZYG-1^{4A}*: zyg-1(it25)*		96.1 ± 3.6	3426
ZYG-1^{S279D}*: zyg-1(it25)*		2.5 ± 2.8	1401
ZYG-1^{4D}*: zyg-1(it25)*		1.9 ± 3.4	1529
wild-type (N2)		100 ± 0	400
ZYG-1^{S279A}		100 ± 0	504
ZYG-1^{4A}		87.7 ± 6.4	457
ZYG-1^{S279D}		97.6 ± 1.2	573
ZYG-1^{4D}		99.1 ± 0.6	336
zyg-1(it25)	23.0	0.3 ± 0.7	716
ZYG-1^{S279A}*: zyg-1(it25)*		3.7 ± 3.1	301
ZYG-1^{4A}*: zyg-1(it25)*		19.7 ± 6.2	514
ZYG-1^{S279D}*: zyg-1(it25)*		0 ± 0	239
ZYG-1^{4D}*: zyg-1(it25)*		0 ± 0	494

Methods and Materials

C. elegans Strains and Genetic Analysis

All strains used in this study were derived from the N2 wild-type strain[70,71]. Animals were maintained at 16 or 19°C on MYOB plates that were seeded with *Escherichia coli* OP50. For embryonic lethality assays, L4 animals were transferred individual plates and allowed to produce progeny for 24-48 h. Progeny were then allowed to develop for 18-24 h before scoring the number of larva and unhatched (dead) embryos. RNAi feeding was performed as previously described[72] using the L4440 empty vector as a negative control. Partial depletion of *rpt-4* was achieved by briefly feeding for 12-18 h prior to imaging. A complete list of *C. elegans* strains that were used in this study is provide in Table S3. Some strains were provided by the CGC, which is funded by NIH Office of Research Infrastructure Programs (P40 OD010440).

CRISPR/Cas9 Genome Editing and Microinjection

Microinjection was performed using the XenoWorks microinjector (Sutter Instruments, Novato, CA) with a continuous pulse setting at 400–800 hPa. For all genome editing, we used the *dpy-10(cn64)* co-CRISPR technique as previously described[73,74]. Animals were microinjected with Cas9 RNP complexes preloaded with equimolar crRNA (0.4-0.8 µg/µl each) and tracrRNA molecules (12 µg/µl) as previously described[75]. Single stranded oligonucleotide repair templates were included at 25-100 ng/µl. Cas9 and custom-designed oligonucleotides (Tables S2, S3) were purchased from IDT (Coralville, IA). Following injection, F1 generation *dpy-10(cn64)* II/+ rollers were screened for each co-edit. All genotypes were verified in homozygous F2 generation animals through Sanger Sequencing (GeneWiz, South Plainfield, NJ).

Expression and purification of recombinant proteins

pGEX-6P-1 plasmids for expressing full length ZYG-1 were provided by Genewiz and transformed into Rosetta 2(DE3) pLysS cells. Starter cultures were inoculated using 2L of LB media and grown at 37°C until the mixture reached an optical density of 0.4-0.6 at 600 nm. Protein expression was induced by adding 1 mM isopropyl ß-D-1-thiogalactopyranoside (IPTG) and incubating the cultures overnight at 16°C (250 rpm). The cells were harvested by centrifugation at 4,000 rcf, and the pellet was resuspended in Lysis Buffer [PBS with 250mM NaCl, 10mM EDTA, 0.1% Tween 20, 200 µg/ml Lysozyme, 0.1% PMSF]. The cells were lysed by sonication at 40% amplitude and a 10s/50s on/off pulse using a 505 Sonic Dismembrator equipped with a ¼" titanium probe (Fisher Scientific). The lysate was then clarified by centrifugation at 18,500 rpm for 1.5 hours using a

Sorvall RC5C Plus centrifuge equipped with a SS34 rotor. The supernatant was then applied to a 10 mL packed GST resin (GE Healthcare, Waukesha, WI) that was equilibrated in Wash Buffer [PBS with 250mM NaCl, and 1 mM DTT]. The column was washed with 3x 20mL volumes of Wash Buffer and the GST fusion proteins were eluted in 50 mM Tris [pH 8.1], 150 mM KCl, and 1mM DTT through a 5-50 mM glutathione gradient. The protein elutions were identified by SDS-PAGE and A280 absorbance, and the samples were dialyzed against Storage Buffer [20mM HEPES pH 7.5, 150mM KCl, 1mM DTT, and 40% Glycerol]. After three exchanges (4 hours each), the concentrated protein samples were snap frozen in liquid nitrogen and stored at -80°C until use.

In vitro Kinase Assays

Recombinant human Casein Kinase 2 (NEB, P6010S) and Protein Kinase A (NEB, P6000S) were purchased from New England Biolabs. Recombinant GST::ZYG-1^{K41M} (kinase-dead)[17] fusion proteins were expressed in *Escherichia coli* and purified using glutathione resin. The GST tag was removed prior to in vitro kinase reactions using PreScission Protease (GenScript, Z02799). Protein concentration was determined using a nanodrop spectrophotometer. For kinase reactions using full-length ZYG-1, 1 µg of recombinant ZYG-1 proteins were incubated with 1 µg of recombinant CK2 in kinase buffer [500 mM Tris-Cl, 100 mM $MgCl_2$, 1 mM EDTA and 20 mM DTT] for 30 minutes at room temperature. Following kinase reactions, proteins were analyzed by SDS/PAGE and autoradiography. ZYG-1 peptides were purchased from Genscript (Piscataway, NJ). For ZYG-1 peptide analysis, 5-10 µg of ZYG-1 peptides were incubated at room temperature for 30 minutes with 1 µg of recombinant CK2 in in kinase buffer [500 mM Tris-Cl, 100 mM $MgCl_2$, 1 mM EDTA and 20 mM DTT]. Peptides were then analyzed through thin layer chromatography and autoradiography as previously described[76]. In brief, the phosphorylated peptides were loaded on silica plates and allowed to chromatograph for 4 h at room temperature. A mixture of n-butanol, acetic acid, pyridine and water (3:1:2:4 ratio) was used as a solvent. For all *in vitro* kinase reactions, 200 µM of cold ATP and 4 µCi of ATP[γ-^{32}P] were included in each reaction. To inhibit CK2 activity, 5 µM TBB (4,5,6,7-tetrabromobenzotriazole, Tocris, 2275) was added to reactions. For mass spectrometry, ZYG-1 peptides following *in vitro* kinase reaction without γ-^{32}P were analyzed for the phosphorylation events by the Taplin Mass Spectrometry facility as described previously[31].

Immunofluorescence and Cytological Analysis

Confocal microscopy was performed as previously described[27], using a Nikon Eclipse Ti-U microscope equipped with a Plan Apo 60× .4 NA lens, a Spinning Disk Confocal (CSU X1) and a Photometrics Evolve 512 camera. The following primary antibodies were used at 1:3000 dilutions: DM1a (Sigma, T9026), α-ZYG-1[56], α-SAS-4[27], α-Myc (ThermoFisher, PA1-981), α-V5 (MBL, M167-3), α-HA (ThermoFisher, 26183) and α-Ollas (ThermoFisher, MA5-16125). Alexa Fluor 488 and 568 secondary antibodies (ThermoFisher, A11001, A11004, A11006, A11034, A11036) were used at 1:3000 dilutions.

Image acquisition and quantification of fluorescence intensity was performed using MetaMorph software (Molecular Devices, Sunnyvale, CA, USA). Adobe Creative Cloud 2023 (Photoshop/Illustrator) was used for image processing. To quantify centrosomal signals, the average intensity within 8 or 9-pixel (1 pixel=0.151 μm) diameter region was recorded for a single focal plane within an area centered on the centrosome. The average intensity within a 25-pixel diameter region drawn outside of the embryo was used for background subtraction.

Immunoprecipitation (IP) and Western Blot

IP experiments were performed as described[56]. Embryos were extracted from adult worms using hypochlorite treatment (1:2:1 ratio of M9 buffer, 5.25% sodium hypochlorite, and 5 M NaOH), washed five times using M9 buffer, frozen in liquid nitrogen and stored at -80°C until use. Embryos were suspended in lysis buffer [50 mM HEPES, pH 7.4, 1 mM EDTA, 1 mM $MgCl_2$, 200 mM KCl, and 10% glycerol (v/v)] supplemented with complete protease inhibitor cocktail (Roche, Basel, Switzerland) and MG132 (Tocris, Avonmouth, Bristol, UK). Embryos were then milled for 5 minutes (repeat x3) at 30 Hz using a Retsch MM 400 mixer-mill (Verder Scientific, Newtown, PA) and sonicated for 3 minutes in an ultrasonic water bath (Thermo Fisher, Waltham, MA).

Lysates were spun at 45,000 rpm for 45 minutes using a Sorvall RC M120EX ultracentrifuge (Thermo Fisher), then the supernatant was recovered to clean tubes. Protein concentrations were determined using a nanodrop spectrophotometer and equivalent amount of total protein lysates was used for IP. Embryonic protein lysates mixed with α-Myc magnetic beads (MBL, M047-11) were incubated by rotation for 1 hour at 4°C and washed (3x 5 minutes) with PBST (PBS + 0.1% Triton-X 100). IP with beads and input samples were resuspended in 2X Laemmli Sample Buffer (Sigma), and boiled for 5 minutes before fractionating on a 4–12% NuPAGE Bis-Tris gel (Invitrogen) and transferred to nitrocellulose membrane. The following antibodies were used at 1:3000-10,000 dilutions: DM1a (Sigma, T9026), α-GFP (Roche, 11814460001), α-V5 (MBL,

M167-3), α-Myc (Genscript, A00704), α-SAS-5[25], IRDye secondary antibodies (LI-COR Biosciences). Blots were imaged using the Odyssey infrared scanner (LI-COR Biosciences) and analyzed using Image Studio software (LI-COR Biosciences).

Statistical analysis

Statistics were generated using R statistical software and presented as average ± standard deviation (SD). Dotplots were generated using the R 'beeswarm' package. In the dotplots, box ranges from the first through third quartile of the data. Thick bar indicates the median. Solid grey line extends 1.5 times the inter-quartile range or to the minimum and maximum data point. All P-values were calculated using two-tailed t-tests: $^{ns}p>0.05$; $^{*}p<0.05$; $^{**}p<0.01$; $^{***}p<0.001$.

References

1. Prigent, C., and Uzbekov, R. (2022). Duplication and Segregation of Centrosomes during Cell Division. Cells *11*, 2445. 10.3390/cells11152445.

2. Marthiens, V., and Basto, R. (2020). Centrosomes: The good and the bad for brain development. Biol Cell *112*, 153–172. 10.1111/boc.201900090.

3. Jaiswal, S., and Singh, P. (2020). Centrosome dysfunction in human diseases. Semin Cell Dev Biol *110*, 113–122. 10.1016/j.semcdb.2020.04.019.

4. Blanco-Ameijeiras, J., Lozano-Fernández, P., and Martí, E. (2022). Centrosome maturation – in tune with the cell cycle. J Cell Sci *135*. 10.1242/jcs.259395.

5. Ong, J.Y., Bradley, M.C., and Torres, J.Z. (2020). Phospho-regulation of mitotic spindle assembly. Cytoskelet Hoboken N J *77*, 558–578. 10.1002/cm.21649.

6. Habedanck, R., Stierhof, Y.-D., Wilkinson, C.J., and Nigg, E.A. (2005). The Polo kinase Plk4 functions in centriole duplication. Nat Cell Biol *7*, 1140–1146. 10.1038/ncb1320.

7. Ohta, M., Ashikawa, T., Nozaki, Y., Kozuka-Hata, H., Goto, H., Inagaki, M., Oyama, M., and Kitagawa, D. (2014). Direct interaction of Plk4 with STIL ensures formation of a single procentriole per parental centriole. Nat Commun *5*, 5267. 10.1038/ncomms6267.

8. Dzhindzhev, N.S., Tzolovsky, G., Lipinszki, Z., Schneider, S., Lattao, R., Fu, J., Debski, J., Dadlez, M., and Glover, D.M. (2014). Plk4 Phosphorylates Ana2 to Trigger Sas6 Recruitment and Procentriole Formation. Curr Biol *24*, 2526–2532. 10.1016/j.cub.2014.08.061.

9. Kratz, A.-S., Bärenz, F., Richter, K.T., and Hoffmann, I. (2015). Plk4-dependent phosphorylation of STIL is required for centriole duplication. Biol Open *4*, 370–377. 10.1242/bio.201411023.

10. Moyer, T.C., Clutario, K.M., Lambrus, B.G., Daggubati, V., and Holland, A.J. (2015). Binding of STIL to Plk4 activates kinase activity to promote centriole assembly. J Cell Biol *209*, 863–878. 10.1083/jcb.201502088.

11. Moyer, T.C., and Holland, A.J. (2019). PLK4 promotes centriole duplication by phosphorylating STIL to link the procentriole cartwheel to the microtubule wall. Elife *8*, e46054. 10.7554/elife.46054.

12. O'Connell, K.F., Caron, C., Kopish, K.R., Hurd, D.D., Kemphues, K.J., Li, Y., and White, J.G. (2001). The C. elegans zyg-1 Gene Encodes a Regulator of Centrosome Duplication with Distinct Maternal and Paternal Roles in the Embryo. Cell *105*, 547–558. 10.1016/s0092-8674(01)00338-5.

13. Woglar, A., Pierron, M., Schneider, F.Z., Jha, K., Busso, C., and Gönczy, P. (2022). Molecular architecture of the C. elegans centriole. Plos Biol *20*, e3001784. 10.1371/journal.pbio.3001784.

14. Pelletier, L., O'Toole, E., Schwager, A., Hyman, A.A., and Müller-Reichert, T. (2006). Centriole assembly in Caenorhabditis elegans. Nature *444*, 619–623. 10.1038/nature05318.

15. Delattre, M., Leidel, S., Wani, K., Baumer, K., Bamat, J., Schnabel, H., Feichtinger, R., Schnabel, R., and Gönczy, P. (2004). Centriolar SAS-5 is required for centrosome duplication in C. elegans. Nat Cell Biol *6*, 656–664. 10.1038/ncb1146.

16. Leidel, S., Delattre, M., Cerutti, L., Baumer, K., and Gönczy, P. (2005). SAS-6 defines a protein family required for centrosome duplication in C. elegans and in human cells. Nat Cell Biol *7*, 115–125. 10.1038/ncb1220.

17. Lettman, M.M., Wong, Y.L., Viscardi, V., Niessen, S., Chen, S., Shiau, A.K., Zhou, H., Desai, A., and Oegema, K. (2013). Direct Binding of SAS-6 to ZYG-1 Recruits SAS-6 to the Mother Centriole for Cartwheel Assembly. Dev Cell *25*, 284–298. 10.1016/j.devcel.2013.03.011.

18. Guderian, G., Westendorf, J., Uldschmid, A., and Nigg, E.A. (2010). Plk4 trans-autophosphorylation regulates centriole number by controlling betaTrCP-mediated degradation. J Cell Sci *123*, 2163–2169. 10.1242/jcs.068502.

19. Holland, A.J., Lan, W., Niessen, S., Hoover, H., and Cleveland, D.W. (2010). Polo-like kinase 4 kinase activity limits centrosome overduplication by autoregulating its own stability. J Cell Biology *188*, 191–198. 10.1083/jcb.200911102.

20. Medley, J.C., DiPanni, J.R., Schira, L., Shaffou, B.M., Sebou, B.M., and Song, M.H. (2021). APC/CFZR-1 regulates centrosomal ZYG-1 to limit centrosome number. J Cell Sci *134*. 10.1242/jcs.253088.

21. Rogers, G.C., Rusan, N.M., Roberts, D.M., Peifer, M., and Rogers, S.L. (2009). The SCF Slimb ubiquitin ligase regulates Plk4/Sak levels to block centriole reduplication. J Cell Biology *184*, 225–239. 10.1083/jcb.200808049.

22. Cunha-Ferreira, I., Rodrigues-Martins, A., Bento, I., Riparbelli, M., Zhang, W., Laue, E., Callaini, G., Glover, D.M., and Bettencourt-Dias, M. (2009). The SCF/Slimb Ubiquitin Ligase Limits Centrosome Amplification through Degradation of SAK/PLK4. Curr Biol *19*, 43–49. 10.1016/j.cub.2008.11.037.

23. Klebba, J.E., Buster, D.W., Nguyen, A.L., Swatkoski, S., Gucek, M., Rusan, N.M., and Rogers, G.C. (2013). Polo-like Kinase 4 Autodestructs by Generating Its Slimb-Binding Phosphodegron. Curr Biol *23*, 2255–2261. 10.1016/j.cub.2013.09.019.

24. Cunha-Ferreira, I., Bento, I., Pimenta-Marques, A., Jana, S.C., Lince-Faria, M., Duarte, P., Borrego-Pinto, J., Gilberto, S., Amado, T., Brito, D., et al. (2013). Regulation of Autophosphorylation Controls PLK4 Self-Destruction and Centriole Number. Curr Biol *23*, 2245–2254. 10.1016/j.cub.2013.09.037.

25. Medley, J.C., Kabara, M.M., Stubenvoll, M.D., DeMeyer, L.E., and Song, M.H. (2016). Casein kinase II is required for proper cell division and acts as a negative regulator of centrosome duplication in Caenorhabditis elegans embryos. Biol Open *6*, 17–28. 10.1242/bio.022418.

26. Kemp, C.A., Song, M.H., Addepalli, M.K., Hunter, G., and O'Connell, K. (2007). Suppressors of zyg-1 Define Regulators of Centrosome Duplication and Nuclear Association in Caenorhabditis elegans. Genetics *176*, 95–113. 10.1534/genetics.107.071803.

27. Song, M.H., Aravind, L., Müller-Reichert, T., and O'Connell, K.F. (2008). The Conserved Protein SZY-20 Opposes the Plk4-Related Kinase ZYG-1 to Limit Centrosome Size. Dev Cell *15*, 901–912. 10.1016/j.devcel.2008.09.018.

28. Miller, J.G., Liu, Y., Williams, C.W., Smith, H.E., and O'Connell, K.F. (2016). The E2F-DP1 Transcription Factor Complex Regulates Centriole Duplication in Caenorhabditis elegans. G3 Genes Genomes Genetics *6*, 709–720. 10.1534/g3.115.025577.

29. Peel, N., Iyer, J., Naik, A., Dougherty, M.P., Decker, M., and O'Connell, K.F. (2017). Protein Phosphatase 1 Down Regulates ZYG-1 Levels to Limit Centriole Duplication. Plos Genet *13*, e1006543. 10.1371/journal.pgen.1006543.

30. Kitagawa, D., Flückiger, I., Polanowska, J., Keller, D., Reboul, J., and Gönczy, P. (2011). PP2A Phosphatase Acts upon SAS-5 to Ensure Centriole Formation in C. elegans Embryos. Dev Cell *20*, 550–562. 10.1016/j.devcel.2011.02.005.

31. Song, M.H., Liu, Y., Anderson, D.E., Jahng, W.J., and O'Connell, K.F. (2011). Protein Phosphatase 2A-SUR-6/B55 Regulates Centriole Duplication in C. elegans by Controlling the Levels of Centriole Assembly Factors. Dev Cell *20*, 563–571. 10.1016/j.devcel.2011.03.007.

32. Brownlee, C.W., Klebba, J.E., Buster, D.W., and Rogers, G.C. (2011). The Protein Phosphatase 2A regulatory subunit Twins stabilizes Plk4 to induce centriole amplification. J Cell Biol *195*, 231–243. 10.1083/jcb.201107086.

33. Hu, E., and Rubin, C.S. (1990). Casein kinase II from Caenorhabditis elegans. Properties and developmental regulation of the enzyme; cloning and sequence analyses of cDNA and the gene for the catalytic subunit. J Biol Chem *265*, 5072–5080. 10.1016/s0021-9258(19)34086-4.

34. Hu, E., and Rubin, C.S. (1991). Casein kinase II from Caenorhabditis elegans. Cloning, characterization, and developmental regulation of the gene encoding the beta subunit. J Biol Chem *266*, 19796–19802. 10.1016/s0021-9258(18)55062-6.

35. Wang, X., Gupta, P., Fairbanks, J., and Hansen, D. (2014). Protein kinase CK2 both promotes robust proliferation and inhibits the proliferative fate in the C. elegans germ line. Dev Biol *392*, 26–41. 10.1016/j.ydbio.2014.05.002.

36. Park, J.-W., Jeong, J., and Bae, Y.-S. (2022). Protein Kinase CK2 Is Upregulated by Calorie Restriction and Induces Autophagy. Mol Cells *45*, 112–121. 10.14348/molcells.2021.0183.

37. Huang, J., Wu, Z., Wang, J., and Zhang, X. (2018). Quantitative phosphoproteomics reveals GTBP-1 regulating C.elegans lifespan at different environmental temperatures. Biochem Bioph Res Co *503*, 1962–1967. 10.1016/j.bbrc.2018.07.142.

38. Groot, R.E.A. de, Rappel, S.B., Lorenowicz, M.J., and Korswagen, H.C. (2014). Protein kinase CK2 is required for Wntless internalization and Wnt secretion. Cell Signal *26*, 2601–2605. 10.1016/j.cellsig.2014.08.016.

39. Li, W.-J., Wang, C.-W., Tao, L., Yan, Y.-H., Zhang, M.-J., Liu, Z.-X., Li, Y.-X., Zhao, H.-Q., Li, X.-M., He, X.-D., et al. (2021). Insulin signaling regulates longevity through protein phosphorylation in Caenorhabditis elegans. Nat Commun *12*, 4568. 10.1038/s41467-021-24816-z.

40. Park, J.-H., Lee, J.-H., Park, J.-W., Kim, D.-Y., Hahm, J.-H., Nam, H.G., and Bae, Y.-S. (2017). Downregulation of protein kinase CK2 activity induces age-related biomarkers in C. elegans. Oncotarget *8*, 36950–36963. 10.18632/oncotarget.16939.

41. Hu, J., Bae, Y.-K., Knobel, K.M., and Barr, M.M. (2006). Casein Kinase II and Calcineurin Modulate TRPP Function and Ciliary Localization. Mol Biol Cell *17*, 2200–2211. 10.1091/mbc.e05-10-0935.

42. Alessi, A.F., Khivansara, V., Han, T., Freeberg, M.A., Moresco, J.J., Tu, P.G., Montoye, E., Yates, J.R., Karp, X., and Kim, J.K. (2015). Casein kinase II promotes target silencing by miRISC through direct phosphorylation of the DEAD-box RNA helicase CGH-1. Proc National Acad Sci *112*, E7213–E7222. 10.1073/pnas.1509499112.

43. Song, J., and Bae, Y.-S. (2021). CK2 Down-Regulation Increases the Expression of Senescence-Associated Secretory Phenotype Factors through NF-κB Activation. Int J Mol Sci *22*, 406. 10.3390/ijms22010406.

44. Litchfield, D.W. (2002). Protein kinase CK2: structure, regulation and role in cellular decisions of life and death. Biochem J *369*, 1–15. 10.1042/bj20021469.

45. Meggio, F., and Pinna, L.A. (2003). One-thousand-and-one substrates of protein kinase CK2? Faseb J *17*, 349–368. 10.1096/fj.02-0473rev.

46. Firnau, M.-B., and Brieger, A. (2022). CK2 and the Hallmarks of Cancer. Biomed *10*, 1987. 10.3390/biomedicines10081987.

47. Pinna, L.A., and Meggio, F. (1997). Protein kinase CK2 ("casein kinase-2") and its implication in cell division and proliferation. Prog Cell Cycle Res *3*, 77–97. 10.1007/978-1-4615-5371-7_7.

48. St-Denis, N.A., Derksen, D.R., and Litchfield, D.W. (2009). Evidence for regulation of mitotic progression through temporal phosphorylation and dephosphorylation of CK2alpha. Mol Cell Biol *29*, 2068–2081. 10.1128/mcb.01563-08.

49. Wolf, B., Balestra, F.R., Spahr, A., and Gönczy, P. (2018). ZYG-1 promotes limited centriole amplification in the C. elegans seam lineage. Dev Biol *434*, 221–230. 10.1016/j.ydbio.2018.01.001.

50. Yim, N., Medley, J.C., and Song, M.H. (2022). The C. elegans Casein Kinase II is associated with meiotic DNA in fertilized oocytes. Micropublication Biology *2022*, 10.17912/micropub.biology.000583. 10.17912/micropub.biology.000583.

51. Salvi, M., Sarno, S., Cesaro, L., Nakamura, H., and Pinna, L.A. (2009). Extraordinary pleiotropy of protein kinase CK2 revealed by weblogo phosphoproteome analysis. Biochimica Et Biophysica Acta Bba - Mol Cell Res *1793*, 847–859. 10.1016/j.bbamcr.2009.01.013.

52. Schwartz, D., and Gygi, S.P. (2005). An iterative statistical approach to the identification of protein phosphorylation motifs from large-scale data sets. Nat Biotechnol *23*, 1391–1398. 10.1038/nbt1146.

53. Ma, R., Li, S., Li, W., Yao, L., Huang, H.-D., and Lee, T.-Y. (2022). KinasePhos 3.0: Redesign and expansion of the prediction on kinase-specific phosphorylation sites. Genom Proteom Bioinform. 10.1016/j.gpb.2022.06.004.

54. Wang, C., Xu, H., Lin, S., Deng, W., Zhou, J., Zhang, Y., Shi, Y., Peng, D., and Xue, Y. (2020). GPS 5.0: An Update on the Prediction of Kinase-specific Phosphorylation Sites in Proteins. Genom Proteom Bioinform *18*, 72–80. 10.1016/j.gpb.2020.01.001.

55. Aebersold, R., and Goodlett, D.R. (2001). Mass Spectrometry in Proteomics. Chem Rev *101*, 269–296. 10.1021/cr990076h.

56. Stubenvoll, M.D., Medley, J.C., Irwin, M., and Song, M.H. (2016). ATX-2, the C. elegans Ortholog of Human Ataxin-2, Regulates Centrosome Size and Microtubule Dynamics. Plos Genet *12*, e1006370. 10.1371/journal.pgen.1006370.

57. Shimanovskaya, E., Viscardi, V., Lesigang, J., Lettman, M.M., Qiao, R., Svergun, D.I., Round, A., Oegema, K., and Dong, G. (2014). Structure of the C. elegans ZYG-1 Cryptic Polo Box Suggests a Conserved Mechanism for Centriolar Docking of Plk4 Kinases. Structure *22*, 1090–1104. 10.1016/j.str.2014.05.009.

58. Kemp, C.A., Kopish, K.R., Zipperlen, P., Ahringer, J., and O'Connell, K.F. (2004). Centrosome Maturation and Duplication in C. elegans Require the Coiled-Coil Protein SPD-2. Dev Cell *6*, 511–523. 10.1016/s1534-5807(04)00066-8.

59. Cundell, M.J., Hutter, L.H., Bastos, R.N., Poser, E., Holder, J., Mohammed, S., Novak, B., and Barr, F.A. (2016). A PP2A-B55 recognition signal controls substrate dephosphorylation kinetics during mitotic exit. J Cell Biol *214*, 539–554. 10.1083/jcb.201606033.

60. Kruse, T., Gnosa, S.P., Nasa, I., Garvanska, D.H., Hein, J.B., Nguyen, H., Samsøe-Petersen, J., Lopez-Mendez, B., Hertz, E.P.T., Schwarz, J., et al. (2020). Mechanisms of site-specific dephosphorylation and kinase opposition imposed by PP2A regulatory subunits. Embo J *39*, e103695. 10.15252/embj.2019103695.

61. Medley, J.C., and Song, M.H. (2023). kin-3 genetically suppresses sur-6 in centrosome assembly during Caenorhabditis elegans embryogenesis. Micropublication Biology *2023*, 10.17912/micropub.biology.000791. 10.17912/micropub.biology.000791.

62. Turowec, J.P., Duncan, J.S., French, A.C., Gyenis, L., Denis, N.A.S., Vilk, G., and Litchfield, D.W. (2010). Protein kinase CK2 is a constitutively active enzyme that promotes cell survival: strategies to identify CK2 substrates and manipulate its activity in mammalian cells. Methods Enzymol *484*, 471–493. 10.1016/b978-0-12-381298-8.00023-x.

63. Zitouni, S., Francia, M.E., Leal, F., Montenegro Gouveia, S., Nabais, C., Duarte, P., Gilberto, S., Brito, D., Moyer, T., Kandels-Lewis, S., et al. (2016). CDK1 Prevents Unscheduled PLK4-STIL Complex Assembly in Centriole Biogenesis. Curr Biol *26*, 1127–1137. 10.1016/j.cub.2016.03.055.

64. Klebba, J.E., Buster, D.W., McLamarrah, T.A., Rusan, N.M., and Rogers, G.C. (2015). Autoinhibition and relief mechanism for Polo-like kinase 4. Proc National Acad Sci *112*, E657–E666. 10.1073/pnas.1417967112.

65. Lopes, C.A.M., Jana, S.C., Cunha-Ferreira, I., Zitouni, S., Bento, I., Duarte, P., Gilberto, S., Freixo, F., Guerrero, A., Francia, M., et al. (2015). PLK4 trans-Autoactivation Controls Centriole Biogenesis in Space. Dev Cell *35*, 222–235. 10.1016/j.devcel.2015.09.020.

66. Čajánek, L., Glatter, T., and Nigg, E.A. (2015). The E3 ubiquitin ligase Mib1 regulates Plk4 and centriole biogenesis. J Cell Sci *128*, 1674–1682. 10.1242/jcs.166496.

67. Yeung, S.-F., Zhou, Y., Zou, W., Chan, W.-L., and Ching, Y.P. (2022). TEC kinase stabilizes PLK4 to promote liver cancer metastasis. Cancer Lett *524*, 70–81. 10.1016/j.canlet.2021.08.038.

68. Nabais, C., Peneda, C., and Bettencourt-Dias, M. (2020). Evolution of centriole assembly. Curr Biol *30*, R494–R502. 10.1016/j.cub.2020.02.036.

69. Carvalho-Santos, Z., Machado, P., Branco, P., Tavares-Cadete, F., Rodrigues-Martins, A., Pereira-Leal, J.B., and Bettencourt-Dias, M. (2010). Stepwise evolution of the centriole-assembly pathway. J Cell Sci *123*, 1414–1426. 10.1242/jcs.064931.

70. Brenner, S. (1974). THE GENETICS OF CAENORHABDITIS ELEGANS. Genetics *77*, 71–94. 10.1093/genetics/77.1.71.

71. Church, D.L., Guan, K.L., and Lambie, E.J. (1995). Three genes of the MAP kinase cascade, mek-2, mpk-1/sur-1 and let-60 ras, are required for meiotic cell cycle progression in Caenorhabditis elegans. Dev Camb Engl *121*, 2525–2535. 10.1242/dev.121.8.2525.

72. Kamath, R.S., Fraser, A.G., Dong, Y., Poulin, G., Durbin, R., Gotta, M., Kanapin, A., Bot, N.L., Moreno, S., Sohrmann, M., et al. (2003). Systematic functional analysis of the Caenorhabditis elegans genome using RNAi. Nature *421*, 231–237. 10.1038/nature01278.

73. Paix, A., Folkmann, A., and Seydoux, G. (2017). Precision genome editing using CRISPR-Cas9 and linear repair templates in C. elegans. Methods *121*, 86–93. 10.1016/j.ymeth.2017.03.023.

74. Arribere, J.A., Bell, R.T., Fu, B.X.H., Artiles, K.L., Hartman, P.S., and Fire, A.Z. (2014). Efficient marker-free recovery of custom genetic modifications with CRISPR/Cas9 in Caenorhabditis elegans. Genetics *198*, 837–846. 10.1534/genetics.114.169730.

75. Paix, A., Folkmann, A., Rasoloson, D., and Seydoux, G. (2015). High Efficiency, Homology-Directed Genome Editing in Caenorhabditis elegans Using CRISPR-Cas9 Ribonucleoprotein Complexes. Genetics *201*, 47–54. 10.1534/genetics.115.179382.

76. Safran, A., Neumann, D., and Fuchs, S. (1986). Analysis of acetylcholine receptor phosphorylation sites using antibodies to synthetic peptides and monoclonal antibodies. Embo J *5*, 3175–3178.

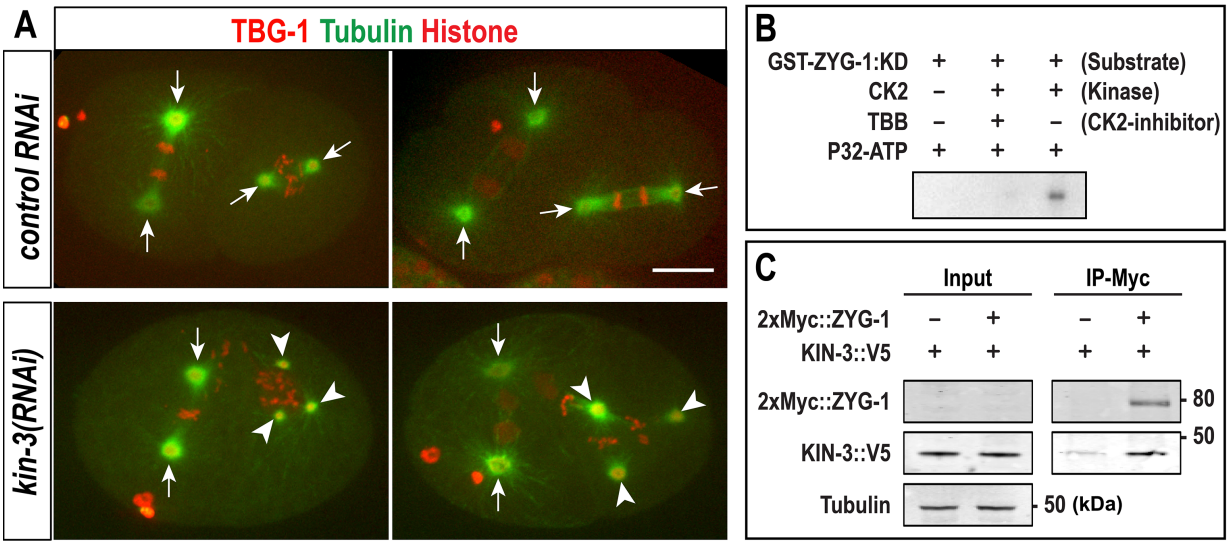

Figure 1. Loss of CK2 leads to extra centrosomes. (A) Still images of embryos expressing GFP::β-tubulin, mCherry::γ-tubulin (TBG-1) and mCherry::histone at the second mitosis. Arrows indicate bipolar spindles and arrowheads illustrate tripolar mitotic spindles. Scale bar, 10μm **(B)** Autoradiogram of GST-ZYG-1 (kinase-dead: KD) incubated with CK2. **(C)** 2xMyc::ZYG-1 co-precipitates with KIN-3::V5. ~5% of total embryonic lysates were loaded in input lanes.

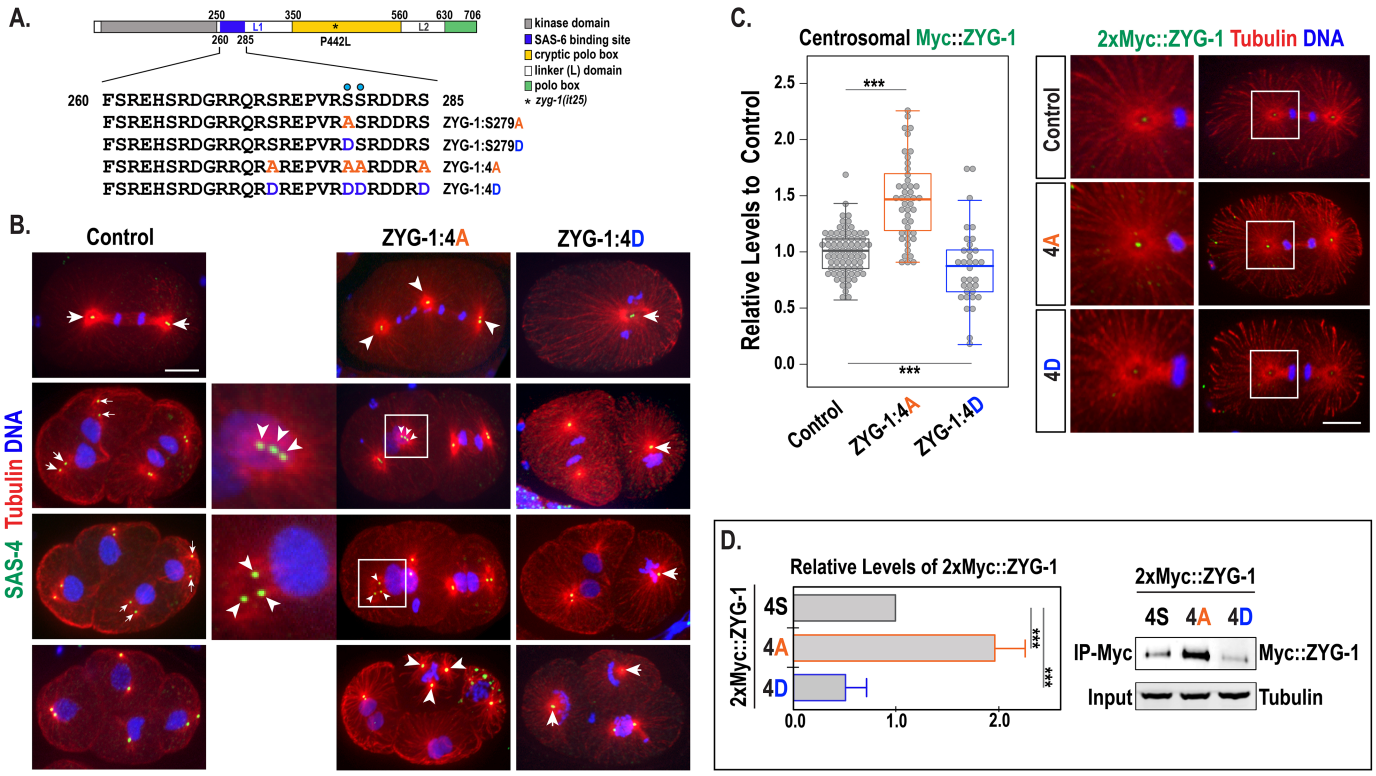

Figure 2. The phosphorylation state of ZYG-1 regulates centrosome number and ZYG-1 stability. **(A)** ZYG-1 protein structure illustrating the locations of functional domains, predicted CK2-dependent phosphorylation sites and phospho-mutations. Blue dots indicate S279 and S280. **(B)** Embryos stained for the centriolar marker SAS-4 (green) and microtubules (red) illustrate abnormal centrosome numbers in ZYG-1 phospho-mutants. While bipolar spindles are always observed in wild-type controls, tripolar spindles are observed in ZYG-1:4A mutants and monopolar spindles in ZYG-1:4D mutants. Insets highlight centrosomes with three centriolar foci stained with SAS-4 at the second telophase (magnified 4-fold). Scale bar, 10μm. **(C)** (Left) Quantification of centrosome-associated 2xMyc::ZYG-1 levels during the first mitotic anaphase. Each dot represents a centrosome. In the plot, box ranges from the first through third quartile of the data. Thick bar indicates the median. Lines extend to the minimum and maximum data point excluding outliers that were defined as beyond 1.5 times the interquartile range. (Right) Centrosomes stained for anti-Myc. Insets highlight centrosomes magnified 4-fold. Scale bar, 10μm. **(D)** (Left) Relative levels of total 2xMyc::ZYG-1 in Myc-pulldown normalized against Tubulin in input lanes (mean ± s.d.). (Right) Immunoprecipitation of 2xMyc::ZYG-1 using Myc-beads. Tubulin was used as a loading control. ~5% of total embryonic lysates were loaded in input lanes. **(C-D)** ***p<0.001 (two-tailed unpaired t-tests).

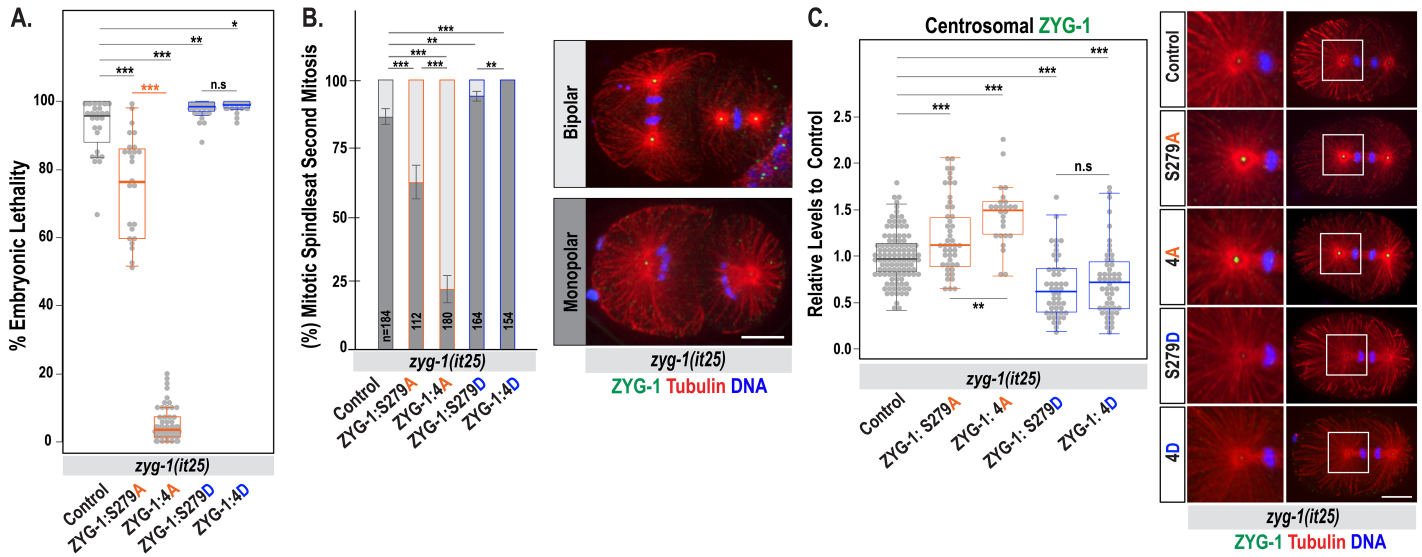

Figure 3. Multisite phosphorylation of ZYG-1 regulates *zyg-1* activity and centrosome duplication (A) Embryonic viability at 23°C (Table 1). Each dot represents a hermaphrodite. **(B)** (Left) Quantification of mitotic spindles at the second mitosis at 23°C (mean ± s.d.). n is the number of blastomeres scored. (Right) Immunostained embryos at the second mitosis illustrate monopolar (dark grey) or bipolar (light grey) spindles. Scale bar, 10µm. **(C)** (Left) Quantification of centrosomal ZYG-1 levels at the first mitotic anaphase. Each dot represents a centrosome. (Right) Embryos stained for ZYG-1 at the first anaphase. Insets highlight centrosomes magnified 4-fold. **(A-C)** n.s $p>0.05$, *$p<0.05$, **$p<0.01$, ***$p<0.001$ (two-tailed unpaired *t*-tests). Boxes ranges from the first through third quartile of the data. Thick bars indicate the median. Lines extend to the minimum and maximum data point excluding outliers that were defined as beyond 1.5 times the interquartile range.

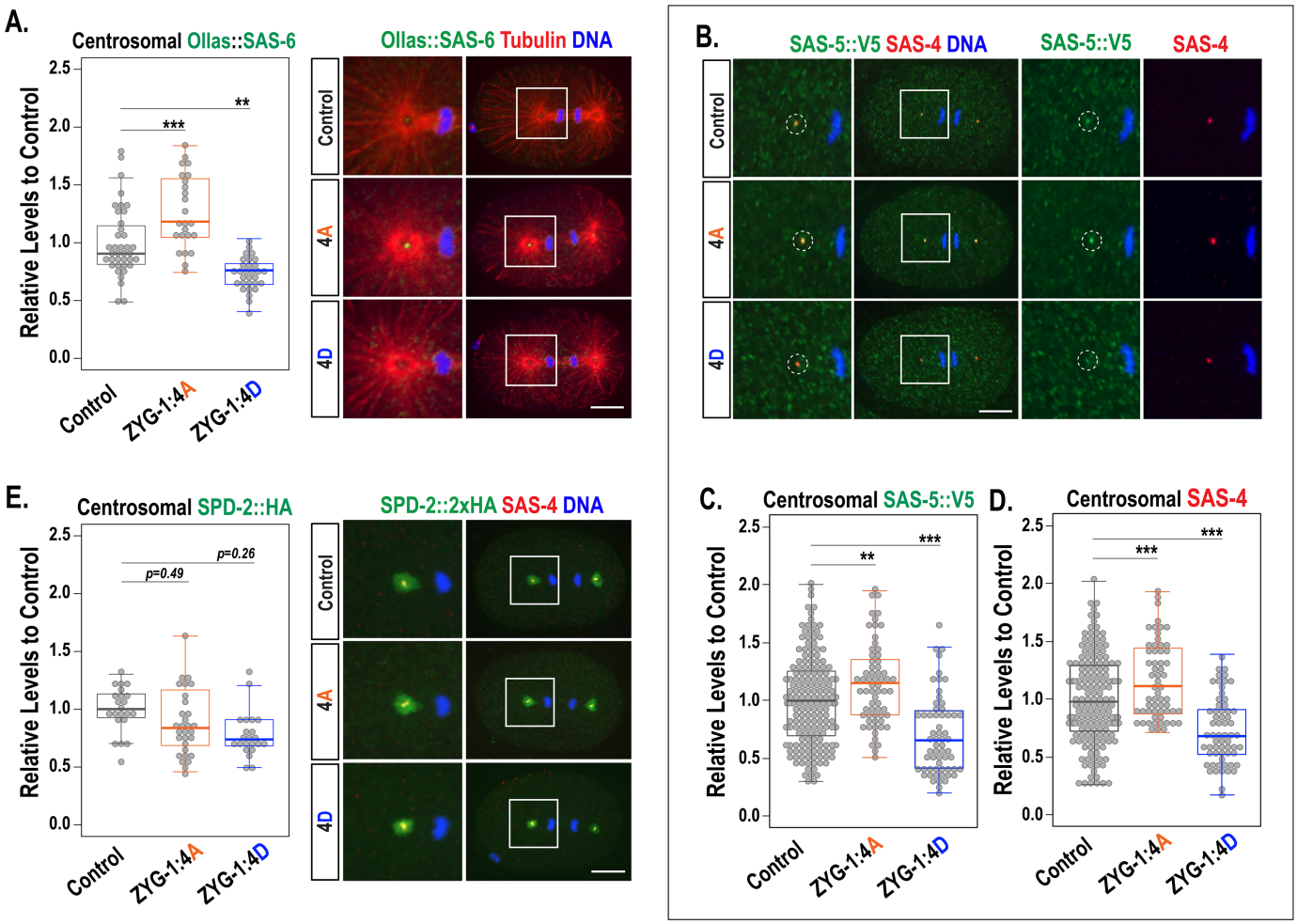

Figure 4. The phosphorylation state of ZYG-1 influences centrosomal levels of downstream factors. ZYG-1 phospho-mutant embryos stained for **(A)** Ollas::SAS-6, **(B)** SAS-5::V5 and SAS-4, **(E)** SPD-2::2xHA. **(B)** The dotted circles highlight co-localization of SAS-5::V5 and SAS-4. Insets highlight centrosomes magnified 4-fold. Scale bar, 10μm. **(A,C-E)** Plots show quantification of centrosomal proteins at the first mitotic anaphase. $^{**}p<0.01$, $^{***}p<0.001$ (two-tailed unpaired *t*-tests). Boxes ranges from the first through third quartile of the data. Thick bars indicate the median. Lines extend to the minimum and maximum data point excluding outliers that were defined as beyond 1.5 times the interquartile range.

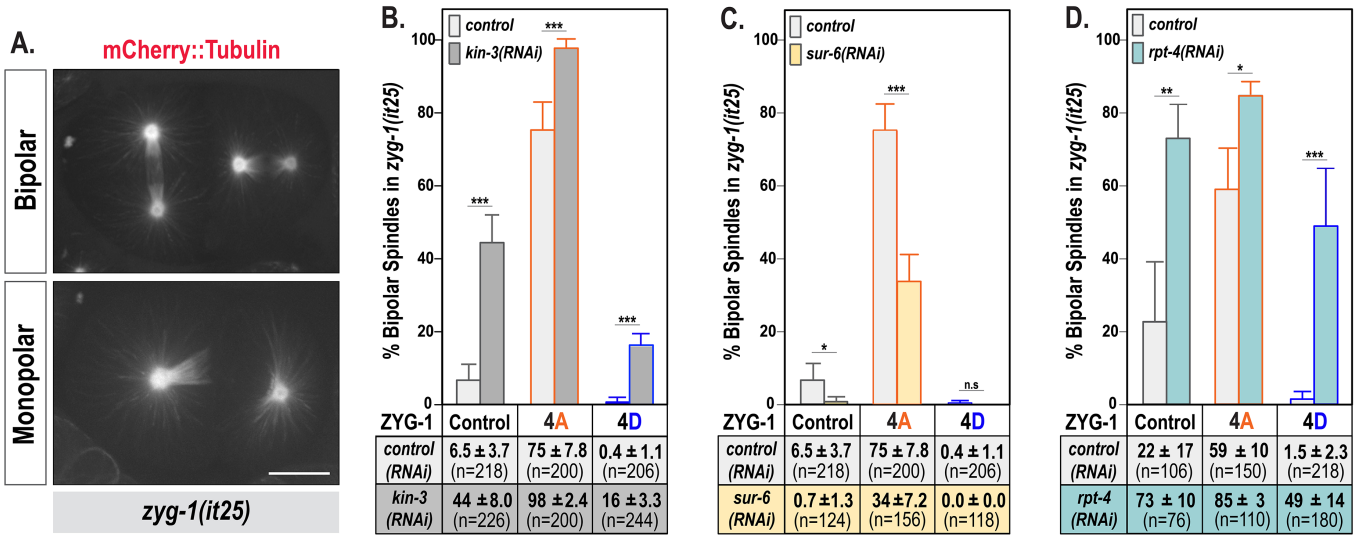

Figure 5. Phosphorylation of ZYG-1 promotes proteasomal degradation of ZYG-1. (A) *zyg-1(it25)* mutant embryos expressing mCherry::Tubulin undergoing the second mitosis illustrate bipolar and monopolar spindles. Scale bar, 10µm. **(B-D)** Quantification of bipolar spindle formation at the second mitosis in *zyg-1(it25)* phospho-mutants at 24°C with knockdown of **(B)** KIN-3, **(C)** SUR-6 or **(D)** RPT-4. (mean ± s.d.). n is the number of blastomeres scored. **p*<0.05, ***p*<0.01, ****p*<0.001 (two-tailed unpaired *t*-tests)